British Journal of Pharmacology (2007) 152, 501–512

0007–1188/07 $30.00
www.brjpharmacol.org

RESEARCH PAPER

Identification of domains influencing assembly and ion channel properties in α7 nicotinic receptor and 5-HT$_3$ receptor subunit chimaeras

VJ Gee, S Kracun, ST Cooper[1], AJ Gibb and NS Millar

Department of Pharmacology, University College London, London, UK

Background and purpose: Nicotinic acetylcholine receptors (nAChRs) and 5-hydroxytryptamine type 3 receptors (5-HT$_3$Rs) are members of the superfamily of neurotransmitter-gated ion channels. Both contain five subunits which assemble to form either homomeric or heteromeric subunit complexes. With the aim of identifying the influence of subunit domains upon receptor assembly and function, a series of chimaeras have been constructed containing regions of the neuronal nAChR α7 subunit and the 5-HT$_3$ receptor $_{3A}$ subunit.
Experimental approach: A series of subunit chimaeras containing α7 and 5-HT$_{3A}$ subunit domains have been constructed and expressed in cultured mammalian cells. Properties of the expressed receptors have been examined by means of radioligand binding, agonist-induced changes in intracellular calcium and patch-clamp electrophysiology.
Key results: Subunit domains which influence properties such as rectification, desensitization and conductance have been identified. In addition, the influence of subunit domains upon subunit folding, receptor assembly and cell-surface expression has been identified. Co-expression studies with the nAChR-associated protein RIC-3 revealed that, in contrast to the potentiating effect of RIC-3 on α7 nAChRs, RIC-3 caused reduced levels of cell-surface expression of some α7/5-HT$_{3A}$ chimaeras.
Conclusions and implications: Evidence has been obtained which demonstrates that subunit transmembrane domains are critical for efficient subunit folding and assembly. In addition, functional characterization of subunit chimaeras revealed that both extracellular and cytoplasmic domains exert a dramatic and significant influence upon single-channel conductance. These data support a role for regions other than hydrophobic transmembrane domains in determining ion channel properties.
British Journal of Pharmacology (2007) **152,** 501–512; doi:10.1038/sj.bjp.0707429; published online 27 August 2007

Keywords: nicotinic receptor; 5-HT receptor; assembly; single-channel conductance

Abbreviations: 5-HT, 5-hydroxytryptamine; 5-HT$_3$R, 5-hydroxytryptamine receptor type 3; αBTX, α-bungarotoxin; CPBG, 1-(3-chlorophenyl)biguanide hydrochloride; DMEM, Dulbecco's modified Eagle's medium; DMPP, 1,1-dimethyl-4-phenylpiperazinium iodide; FCS, fetal calf serum; FLIPR, fluorometric imaging plate reader; HBSS, Hanks' buffered saline solution; nAChR, nicotinic acetylcholine receptor

Introduction

Nicotinic acetylcholine receptors (nAChRs) are pentameric ligand-gated ion channels which exhibit considerable subunit diversity (Le Novère *et al*., 2002; Millar, 2003; Alexander *et al*., 2007). In addition to nAChR subunits expressed at the neuromuscular junction (α1, β1, γ, δ and ε), 12 neuronal nAChR subunits (α2–α10 and β2–β4) have been identified which coassemble to generate a diverse family of neuronal nAChRs.

While most nAChRs are heteromeric complexes (containing two or more distinct subunit types), there is evidence that some native nAChRs, such as those containing the α7 subunit, are homomeric (Chen and Patrick, 1997; Drisdel and Green, 2000). Homomeric α7 nAChRs are widely distributed in the brain and are now recognized to have an important physiological role as presynaptic receptors, particularly in the reward pathways that may be important in nicotine addiction (Clarke, 1992; MacDermott *et al*., 1999). Although the α7 subunit has been shown to generate functional homomeric nAChRs when expressed in *Xenopus* oocytes (Couturier *et al*., 1990), considerable difficulties have been encountered in attempts to generate functional nAChRs by heterologous expression of α7 in a range of mammalian cell types (Cooper and Millar, 1997; Kassner and Berg, 1997; Rangwala *et al*., 1997). In contrast, such

Correspondence: Dr NS Millar, Department of Pharmacology, University College London, Gower Street, London WC1E 6BT, UK.
E-mail: n.millar@ucl.ac.uk
[1]Current address: The Institute for Neuromuscular Research, The Children's Hospital at Westmead, Westmead NSW 2145, Sydney, Australia
Received 9 May 2007; revised 26 June 2007; accepted 2 July 2007; published online 27 August 2007

difficulties have not been encountered in heterologous expression of homomeric 5-hydroxytryptamine (5-HT, serotonin) type 3 receptors (5-HT$_3$Rs). Heterologous expression of the 5-HT$_{3A}$ subunit results in efficient formation of functional 5-HT$_3$Rs in all cell types which have been examined (Maricq *et al*., 1991; Hargreaves *et al*., 1994; Cooper and Millar, 1997). Similarly, a subunit chimaera containing the extracellular domain of the α7 subunit and the transmembrane and intracellular domains of the 5-HT$_{3A}$ subunit generates high levels of functional cell-surface receptors in all cell lines tested, including cells in which α7 fails to do so (Eiselé *et al*., 1993; Blumenthal *et al*., 1997; Rangwala *et al*., 1997; Cooper and Millar, 1998). These findings have suggested that inefficient folding or assembly of the α7 subunit can be attributed to sequences present within the C-terminal (transmembrane and intracellular) region, a conclusion which is supported by studies conducted with other subunit chimaeras (Campos-Caro *et al*., 1996; Cooper and Millar, 1998; Cooper *et al*., 1999; Quiram and Sine, 1998; Baker *et al*., 2004; Lansdell and Millar, 2004).

In the present study, we have generated a series of subunit chimaeras containing regions of the nAChR α7 subunit and the 5-HT$_{3A}$ subunit. By heterologous expression of these chimaeras, we have identified nAChR subunit domains which markedly influence folding, assembly, cell-surface expression and ion-channel properties.

Methods

Plasmids and cDNAs

The rat nAChR α7 subunit cDNA (Séguéla *et al*., 1993) was provided by Jim Patrick (Baylor College of Medicine, TX). The mouse 5-HT$_{3A}$ subunit cDNA (Maricq *et al*., 1991) was provided by David Julius (University of California, San Francisco, CA, USA). Cloning of the human RIC-3 cDNA has been described previously (Lansdell *et al*., 2005).

Construction of α7/5-HT$_{3A}$ subunit chimaeras

Subunit chimaeras (Figure 1) were constructed from the rat nAChR α7 (Séguéla *et al*., 1993) and mouse 5-HT$_{3A}$ subunit cDNAs (Maricq *et al*., 1991). The α7$^{(V201)}$/5-HT$_{3A}$ chimaera (here referred to as α7$^{V201\text{-}5HT3A}$) has been described previously (Eiselé *et al*., 1993; Cooper and Millar, 1998). Three further α7/5-HT$_{3A}$ subunit chimaeras (α7$^{S235\text{-}5HT3A}$, α7$^{D265\text{-}5HT3A}$ and α7$^{G301\text{-}5HT3A}$) were constructed, each of which contained an N-terminal α7 domain and a C-terminal 5-HT$_{3A}$ domain. Chimaera α7$^{S235\text{-}5HT3A}$ was constructed by introducing a *Bsp*EI site at a position corresponding to Ser^{235} in α7 and Ser^{251} in 5-HT$_{3A}$. Chimaera α7$^{D265\text{-}5HT3A}$ was constructed by introducing a *Kpn*I site at Asp^{265} in α7 and an existing *Kpn*I site at Gly^{280} in 5-HT$_{3A}$. Chimaera α7$^{G301\text{-}5HT3A}$ was constructed by introducing a *Bsp*120I site at Gly^{301} in α7 and an existing *Eae*I site at Arg^{316} in 5-HT$_{3A}$. A chimaera in which the TM1 domain of α7 was replaced by the corresponding region of the 5-HT$_{3A}$ subunit (α7$^{1TM\text{-}5HT3A}$) was constructed by subcloning a fragment of the α7$^{V201\text{-}5HT3A}$ chimaera from a *Hind*III site in the multiple cloning site before the cDNA, to a *Bsp*EI site introduced after TMI (at Ser^{235}) into a *Hind*III site (before the cDNA) and a *Bsp*EI site (introduced by site-directed mutagenesis at Ser^{235}) in α7. A chimaera in which the TM1 and TM2 domains of α7 were replaced by the corresponding regions of the 5-HT$_{3A}$ subunit (α7$^{2TM\text{-}5HT3A}$) was constructed by subcloning 5-HT$_{3A}$ cDNA from the endogenous *Bcl*I site in 5-HT$_{3A}$ and a *Kpn*I site introduced into 5-HT$_{3A}$ at Gly^{280} into a *Bcl*I (Val^{201}) site and a *Kpn*I (Asp^{265}) site in α7. A chimaera in which the TM1–TM3 domains of α7 were replaced by the corresponding regions of the 5-HT$_{3A}$ subunit (α7$^{3TM\text{-}5HT3A}$) was constructed by subcloning 5-HT$_{3A}$ cDNA from the endogenous *Bcl*I site in 5-HT$_{3A}$ and an *Eag*I site introduced into 5-HT$_{3A}$ at Arg^{316} into a *Bcl*I (Val^{201}) site and a *Bsp*120I (Gly^{301}) site in α7. A chimaera in which the TM1-TM3 and TM4 domains of α7 were replaced by the corresponding regions of the 5-HT$_{3A}$ subunit (α7$^{4TM\text{-}5HT3A}$) was constructed by annealing complementary PCR fragments amplified from α7$^{3TM\text{-}5HT3A}$ and 5-HT$_{3A}$ corresponding to the region just before the fourth transmembrane domain, and DNA polymerase I was used for elongation resulting in a change from α7 (at Val^{443}) to 5-HT$_{3A}$ (at Val^{433}). A chimaera in which the TM3-TM4 intracellular loop of α7 was replaced with the corresponding region of 5-HT$_{3A}$ (α7$^{3\text{-}4Loop\text{-}5HT3A}$) was constructed by introducing an *Xba*I site at Leu^{419} in the α7$^{G301\text{-}5HT3A}$ chimaera and Val^{444} in the α7 subunit DNA. A chimaera in which the TM3–TM4 loop of 5-HT$_{3A}$ was replaced with the corresponding region of α7 (5-HT$_{3A}$$^{3\text{-}4Loop\text{-}α7}$) was constructed by using an *Acc*I site at the position Val^{286} in 5-HT$_{3A}$ and Val^{271} in α7$^{4TM\text{-}5HT3A}$. A chimaera in which the M1 and M4 domains of α7 were replaced with the corresponding regions of the 5-HT$_{3A}$ subunit (α7$^{1\&4TM\text{-}5HT3A}$) was constructed by introducing a *Bst*Z17I site into both α7$^{1TM\text{-}5HT3A}$ and α7$^{4TM\text{-}5HT3A}$ at position Val^{443}. A chimaera in which the M1, M2 and M4 domains of α7 were replaced with the corresponding regions of the 5-HT$_{3A}$ subunit (α7$^{1,2\&4TM\text{-}5HT3A}$) was constructed by introducing a *Bst*Z17I site into both α7$^{2TM\text{-}5HT3A}$ and α7$^{4TM\text{-}5HT3A}$ at position Val^{443}. A chimaera in which the M1 and M3-M4 domains of α7 were replaced with the corresponding regions of the 5-HT$_{3A}$ subunit (α7$^{1TM\&D265\text{-}5HT3A}$) was constructed by introducing a *Kpn*I site into α7$^{1TM\text{-}5HT3A}$ at position Ser^{266}, and subcloning into a *Kpn*I site in α7$^{D265\text{-}5HT3A}$.

Heterologous expression in human embryonic kidney tsA201 cells

Human embryonic kidney tsA201 cells were cultured in Dulbecco's modified Eagle's medium (DMEM) containing 2 mM L-Glutamax (Gibco-Invitrogen, Paisley, UK) and 10% heat-inactivated fetal calf serum (FCS) (Sigma, Poole, UK) at 37°C. Cells were transfected using the Effectene transfection kit (Qiagen, Crawley, UK) according to the manufacturer's instructions.

Radioligand binding

Radioligands [^{125}I]α-bungarotoxin ([^{125}I]αBTX; specific activity 7.4 TBq mmol^{-1}) and [^{3}H]GR65630 (specific activity 2.78 TBq mmol^{-1}) were purchased from GE Healthcare (Little Chalfont, UK) and Perkin Elmer (Seer Green, UK), respectively. For both whole-cell and cell membranes, cell monolayers were rinsed and collected in Hanks' buffered saline

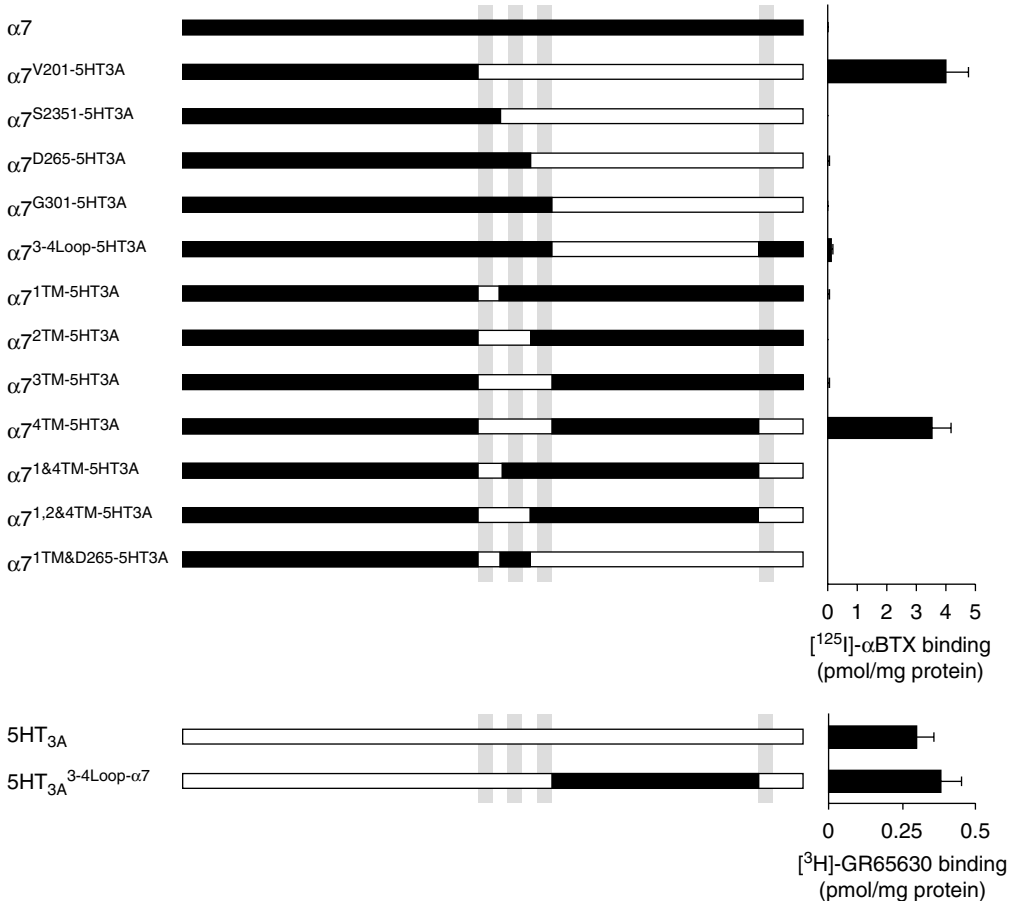

Figure 1 Radioligand binding to α7/5-HT$_{3A}$ subunit chimaeras. Subunit chimaeras containing nAChR α7 subunit domains (black bars) and 5-HT$_{3A}$ subunit domains (white bars) are illustrated (not to scale). Grey bars indicate the positions of the four hydrophobic transmembrane domains (M1–M4). Wild-type and chimaeric subunits were expressed in tsA201 cells and membrane preparations assayed for specific binding of nAChR or 5-HT$_3$R radioligands ([^{125}I]αBTX and [^{3}H]GR65630). Specific radioligand binding is presented as a mean of 6–9 independent experiments, each performed in triplicate. No significant difference was seen in levels of [^{125}I]αBTX binding to α7$^{V201\text{-}5HT3A}$ and α7$^{4TM\text{-}5HT3A}$ or of [^{3}H]GR65630 binding to 5-HT$_{3A}$ and 5-HT$_{3A}$$^{3\text{-}4Loop\text{-}\alpha7}$. nAChR, nicotinic acetylcholine receptor; [^{125}I]αBTX, α-bungarotoxin; 5-HT$_3$R, 5-hydroxytryptamine receptor type 3.

solution (HBSS) and pelleted by gentle centrifugation. Cell membranes were prepared by freeze/thawing of cell pellets and were resuspended in phosphate buffer containing protease inhibitors (4 μg ml^{-1} pepstatin, 8 μg ml^{-1} leupeptin, 8 μg ml^{-1} aprotinin), transferred to 5 ml polystyrene assay tubes and incubated with radioligand (15 nM αBTX (5 nM [^{125}I]αBTX and 10 nM unlabelled αBTX) or 10 nM [^{3}H]GR65630) for 2 h, shaking, on ice. In the case of αBTX binding, 2.5% bovine serum albumin was added to the assay. Non-specific binding of [^{3}H]GR65630 was determined with 12.5 mM 5-HT and of [^{125}I]αBTX binding with 1.25 mM nicotine and 1.25 mM carbachol. For cell-surface [^{125}I]αBTX binding, cells were prepared as above except, after pelleting, cells were resuspended by gentle agitation and pipetting, and assayed in HBSS (containing protease inhibitors, as above) at room temperature. [^{125}I]αBTX and [^{3}H]GR65630-labelled samples were harvested using a Brandel cell harvester (Model M36, Semat, St Albans, UK) onto Whatman GF/A and Whatman GF/B filters, respectively, pre-soaked in 0.5% w v^{-1} polyethylene-imine. Radioactive counts were assayed in a gamma counter (Wallac 1261 Multigamma) for [^{125}I]αBTX binding and by a scintillation counter (Beckman LS 6500) for [^{3}H]GR65630 binding.

Intracellular calcium assay

Transfected cells were replated onto poly-L-lysine-coated black-walled 96-well plates (Marathon Laboratories, London, UK) approximately 18–20 h post transfection. Approximately 24 h after plating, media were removed and the cells incubated in the calcium-sensitive dye Fluo-4. Approximately 50–100 μl of Fluo-4 acetoxymethyl ester (Invitrogen-Molecular Probes, Paisley, UK) at a concentration of 1 μM was added in HBSS with 0.02% Pluronic F-127 (Invitrogen-Molecular Probes, Paisley, UK) for 30–60 min at room temperature. Cells were rinsed 1–2 times, in either HBSS or Tyrode's buffer and assayed using a fluorometric imaging plate reader (FLIPR) in either HBSS or Tyrode's buffer (Molecular Devices, Wokingham, UK). Agonist-induced channel opening and subsequent changes in intracellular calcium was assayed by monitoring changes in fluorescence intensity of the calcium-sensitive dye. Cells were excited at

488 nm and the emitted fluorescence passed through a 510–570 nm band-pass interference filter before detection with a cooled CCD camera. Drug dilutions were prepared in a separate 96-well plate delivered via an automated 96-tip pipettor. Fluorescence measurements were recorded simultaneously for all 96 wells at 1 s intervals, typically for 160 s, with agonist additions after 25 s. Average fluorescence intensity readings before agonist applications were subtracted and data presented as changes in fluorescence intensity in arbitrary units.

Electrophysiology

Cells, grown on glass coverslips coated in collagen and polylysine (both 10 μg ml^{-1}), were co-transfected with pEGFP-C2 (Clontech, Mountain View, CA, USA), encoding green fluorescent protein, and plasmids containing either wild-type or chimaeric subunit cDNA in the ratio of 1:20. Whole-cell recordings were performed at room temperature, 36–48 h after transfection. Recording solution contained (in mM): 110 NaCl, 5.4 KCl, 0.8 $MgCl_2$, 1.8 $CaCl_2$, 25 glucose, 0.9 NaH_2PO_4, 44 $NaHCO_3$. Borosilicate electrodes (GC150F-7.5; Harvard Apparatus, Edenbridge, UK) of resistance 2–8 MΩ contained (in mM) 140 CsCl, 10 HEPES, 10 EGTA, 0.5 $CaCl_2$, 29.53 CsOH, pH adjusted to 7.26, osmolarity 283 mOsm kg^{-1} H_2O. Unless otherwise specified, the holding potential was −60 mV. Fast cell superfusion was achieved with a θ-barrelled application pipette made from 1.5 mm diameter θ tubing (AH-30-0114; Harvard Apparatus, Edenbridge, UK), which was moved laterally using a stepper motor. Applications (20 s) of ACh, 1-(3-chlorophenyl)biguanide hydrochloride (CPBG), 1,1-dimethyl-4-phenylpiperazinium iodide (DMPP) or 5-HT were made and the evoked currents recorded using an Axopatch 200B amplifier. These were stored on magnetic or digital audio tape for subsequent analysis or digitized online at 10 kHz using WinEDR (Strathclyde Electrophysiology Software; www.strath.ac.uk/Departments/PhysPharm) after filtering and further amplification to provide a low-gain OHz−2 kHz record that was used to measure the agonist-induced mean current. The kinetics of desensitization were analysed on 20 s agonist applications. Responses were inverted and fitted with one or the sum of two exponential functions to measure the time constants (τ) and the percentage desensitization after 20 s. A high-gain band-pass (2 Hz−2 kHz butterworth filter) recording was used for variance and spectral density analysis. The recording was divided into segments of 0.82 s duration and edited to remove any segments with obvious artefacts. A 10% cosine taper window was applied to each segment and the single-sided spectral density computed by fast Fourier transform and averaged over 16–32 logarithmically spread frequency ranges. The mean background spectrum was subtracted from the mean spectrum in the presence of the agonist to give the net agonist-induced noise spectrum. The single-channel conductance was calculated from the variance of the noise and from the integration of the net power spectrum fitted with a single or the sum of two lorentzian components as appropriate (Dempster, 2001). For two-component spectra, a weighted noise time constant was calculated from $\tau_w = \tau_1 A_1 + \tau_2 A_2$, where A_1 and A_2 are the relative areas of each Lorentzian component. Rectification was investigated over the voltage range from −60 to +40 mV in 10 mV steps using three 500 ms agonist applications at 10-s intervals every minute. The size of agonist responses was verified at −40 and −60 mV after the final response at +40 mV.

Statistics

Student's paired or unpaired *t*-test, as appropriate, was used with unequal sample variance. For multiple comparisons, ANOVA with Tukey's multiple comparison for unequal sample sizes was used.

Chemicals

The following chemicals (all from Sigma-Aldrich, Poole, UK) were used: CPBG, 5-HT, acetylcholine (ACh), DMPP. Stock solutions were prepared in water and stored frozen.

Results

Human embryonic kidney tsA201 cells were transfected with the nAChR α7 subunit and with a previously described subunit chimaera, α7$^{V201\text{-}5HT3A}$ (Cooper and Millar, 1998), which contains the N-terminal extracellular domain of the nAChR α7 subunit together with the C-terminal (intracellular and transmembrane) domain of 5-HT$_{3A}$. As has been reported previously (Eiselé *et al.*, 1993; Blumenthal *et al.*, 1997; Rangwala *et al.*, 1997; Cooper and Millar, 1998), high levels of [^{125}I]αBTX binding were detected in cells transfected with α7$^{V201\text{-}5HT3A}$ subunit chimaera (4.9 ± 1.0 pmol mg^{-1} protein, $n = 6$; Figure 1). In contrast, no specific binding of [^{125}I]αBTX was detected in cells transfected with α7 (Figure 1).

With the aim of identifying more precisely subunit domains influencing nAChR folding and assembly, several further α7/5-HT$_{3A}$ subunit chimaeras were constructed (Figure 1). Chimaeric subunits were expressed in tsA201 cells and examined for their ability to form a high-affinity binding site for [^{125}I]αBTX. As illustrated in Figure 1, no specific binding of [^{125}I]αBTX was detected in cells transfected with α7/5-HT$_{3A}$ chimaeras containing an N-terminal α7 subunit domain that was fused to the C-terminal domain 5-HT$_{3A}$ after transmembrane region M3 (α7$^{G301\text{-}5HT3A}$), M2 (α7$^{D265\text{-}5HT3A}$) or M1 (α7$^{S235\text{-}5HT3A}$).

Additional α7/5-HT$_{3A}$ subunit chimaeras were constructed which contained the entire α7 sequence, except for selected transmembrane domains derived from the analogous regions of 5-HT$_{3A}$ (α7$^{1TM\text{-}5HT3A}$, α7$^{2TM\text{-}5HT3A}$, α7$^{3TM\text{-}5HT3A}$, α7$^{4TM\text{-}5HT3A}$, Figure 1). Chimaeras containing the M1 region of 5-HT$_{3A}$ (α7$^{1TM\text{-}5HT3A}$), M1–M2 region of 5-HT$_{3A}$ (α7$^{2TM\text{-}5HT3A}$) or the M1–M3 region (α7$^{3TM\text{-}5HT3A}$) showed little or no specific [^{125}I]αBTX binding (Figure 1). In contrast, expression of a chimaera (α7$^{4TM\text{-}5HT3A}$) which contained all four of the predicted transmembrane domains from 5-HT$_{3A}$, but containing the N-terminal and the large intracellular loop of α7, resulted in high levels of specific [^{125}I]αBTX binding (3.5 ± 0.7 pmol mg^{-1} protein, $n = 6$; Figure 1), similar to that

observed with $\alpha7^{V201\text{-}5HT3A}$. These findings demonstrate that efficient subunit folding and assembly (as assayed by [^{125}I]αBTX binding) is possible in tsA201 cells only for those subunits examined which contain all four transmembrane domains from 5-HT$_{3A}$ ($\alpha7^{V201\text{-}5HT3A}$ and $\alpha7^{4TM\text{-}5HT3A}$). To examine whether this was a valid conclusion, three additional chimaeras ($\alpha7^{1\&4TM\text{-}5HT3A}$, $\alpha7^{1,2\&4TM\text{-}5HT3A}$ and $\alpha7^{1TM\&D265\text{-}5HT3A}$) were constructed which contained combinations of TM domains derived from α7 and 5-HT$_{3A}$ (Figure 1). In all cases, no significant binding of [^{125}I]αBTX was detected.

Radioligand binding studies were also performed with intact transfected cells to examine whether specific [^{125}I]αBTX binding could be detected on the cell surface. High levels of cell-surface [^{125}I]αBTX binding were detected in cells transfected with either $\alpha7^{V201\text{-}5HT3A}$ or $\alpha7^{4TM\text{-}5HT3A}$ (3.5 ± 0.5 and 2.7 ± 0.5 pmol mg^{-1} protein, respectively; $n=6$). No significant surface binding of [^{125}I]αBTX could be detected with α7 or with the other subunit chimaeras containing an α7 extracellular domain.

To examine further the influence of the large intracellular loop, two additional chimaeras ($\alpha7^{3\text{-}4Loop\text{-}5HT3A}$ and 5-HT$_{3A}{}^{3\text{-}4Loop\text{-}\alpha7}$) were constructed (Figure 1). No [^{125}I]αBTX binding was detected in cells transfected with $\alpha7^{3\text{-}4Loop\text{-}5HT3A}$ (Figure 1), but high levels of specific binding of the 5-HT$_{3A}$ receptor ligand [^{3}H]GR65630 were detected in cells transfected with 5-HT$_{3A}{}^{3\text{-}4Loop\text{-}\alpha7}$ (0.38 ± 0.07 pmol mg^{-1} protein, $n=9$; Figure 1).

Recent evidence has indicated that difficulties in the efficient expression of α7 in cultured mammalian cell lines (including tsA201 cells) can be overcome by co-expression of the nAChR-associated protein RIC-3 (Castillo *et al*., 2005; Lansdell *et al*., 2005; Williams *et al*., 2005). The present study suggests that in the absence of RIC-3, the transmembrane regions of α7 are responsible for inefficient folding and cell-surface expression. As we have reported previously, when α7 is co-expressed with RIC-3 in tsA201 cells, high levels of cell-surface [^{125}I]αBTX binding is detected (Lansdell *et al*., 2005). In addition, co-expression of RIC-3 permits functional expression of α7 nAChRs, as demonstrated by patch-clamp electrophysiology (Lansdell *et al*., 2005). We examined whether co-expression of RIC-3 modulated levels of cell-surface [^{125}I]αBTX binding to α7/5-HT$_{3A}$ subunit chimaeras. In contrast to the dramatic effect of RIC-3 on levels of [^{125}I]αBTX binding to the α7 subunit (Lansdell *et al*., 2005), none of the α7/5-HT$_{3A}$ subunit chimaeras showed significantly increased levels of [^{125}I]αBTX binding when co-expressed with RIC-3 (data not shown). In fact, a substantial reduction in the level of cell-surface [^{125}I]αBTX binding was observed when RIC-3 was co-expressed with $\alpha7^{V201\text{-}5HT3A}$ and $\alpha7^{4TM\text{-}5HT3A}$ chimaeras. The level of cell-surface [^{125}I]αBTX binding detected when these chimaeras were co-expressed with RIC-3 was substantially lower than the level detected in the absence of RIC-3. The levels of [^{125}I]αBTX binding detected when chimaeras were co-expressed with RIC-3 were only $5\pm2.9\%$; $n=3$ (for $\alpha7^{V201\text{-}5HT3A}$) and $28\pm8.3\%$; $n=5$ (for $\alpha7^{4TM\text{-}5HT3A}$). In paired experiments, the levels of cell-surface [^{125}I]αBTX binding determined in the absence of RIC-3 were 673 ± 83 fmol mg^{-1} for $\alpha7^{V201\text{-}5HT3A}$ and 723 ± 219 fmol mg-1 for $\alpha7^{4TM\text{-}5HT3A}$.

The experiments described provide strong evidence for the role of discrete subunit domains as determinants of the ability of subunit proteins to form correctly folded ligand-binding sites but do not address the question of whether these subunit chimaeras are able to generate functional agonist-gated ion channels. To examine this question, chimaeras were examined by means of an intracellular calcium FLIPR assay (Figures 2a and b). Clear evidence of functional responses were observed for $\alpha7^{V201\text{-}5HT3A}$, $\alpha7^{4TM\text{-}5HT3A}$, 5-HT$_{3A}{}^{3\text{-}4Loop\text{-}\alpha7}$ and 5-HT$_{3A}$, indicating a correlation between high-affinity radioligand binding (Figure 1) and functional expression. These constructs were, therefore, investigated further using whole-cell patch-clamp recording from tsA201 cells transfected with each of the four subunits (or subunit chimaeras) for which specific radioligand binding had been detected. In each case, functional responses to rapid agonist application were obtained, as illustrated (Figure 2c). Figure 2c shows a representative recording from a single cell transfected with the 5-HT$_{3A}{}^{3\text{-}4Loop\text{-}\alpha7}$ chimaera. The responses evoked by rapid applications of CPBG (1 μM for 500 ms) are illustrative of those used to construct the current–voltage relations presented in Figure 3. As would be expected from the presence of the N-terminal region of α7 in $\alpha7^{V201\text{-}5HT3A}$ and $\alpha7^{4TM\text{-}5HT3A}$, both of these chimaeras gave responses to nicotinic agonists (ACh and DMPP). Similarly, 5-HT$_{3A}{}^{3\text{-}4Loop\text{-}\alpha7}$ and 5-HT$_{3A}$ gave responses to 5-HT$_3$ receptor agonists (5-HT and CPBG).

All of the subunits for which radioligand binding was detected, and for which functional expression has been confirmed ($\alpha7^{V201\text{-}5HT3A}$, $\alpha7^{4TM\text{-}5HT3A}$, 5-HT$_{3A}{}^{3\text{-}4Loop\text{-}\alpha7}$ and 5-HT$_{3A}$), contain identical hydrophobic transmembrane domains (M1, M2, M3 and M4) from 5-HT$_{3A}$. Consequently, they might be expected to exhibit similar, if not identical, ion channel properties (see Discussion). The reversal potential and rectification of the four subunit constructs was investigated and were found to be not significantly different (Figure 3 and Table 1). These functional characteristics are much more similar to those shown previously for the 5-HT$_{3A}$ receptor (Gunthorpe *et al*., 2000) than for the α7 subunit (Zhao *et al*., 2003) and suggest that current rectification is a property determined mainly by the transmembrane regions (see also data presented below in which the ion channel properties of α7 co-expressed with RIC-3 have been examined). Examination of the kinetics of desensitization (Figure 4 and Table 1) revealed a significant difference between the two subunit chimaeras containing an α7-extracellular domain ($\alpha7^{V201\text{-}5HT3A}$ and $\alpha7^{4TM\text{-}5HT3A}$) and those constructs with a 5-HT$_{3A}$-extracellular domain (5-HT$_{3A}{}^{3\text{-}4Loop\text{-}\alpha7}$ and 5-HT$_{3A}$). The time constant for decay was significantly smaller ($P<0.05$) for $\alpha7^{V201\text{-}5HT3A}$ and $\alpha7^{4TM\text{-}5HT3A}$ than for 5-HT$_{3A}{}^{3\text{-}4Loop\text{-}\alpha7}$ and 5-HT$_{3A}$. Similarly, the percentage desensitization after 20 s was significantly less ($P<0.05$) for $\alpha7^{V201\text{-}5HT3A}$ and $\alpha7^{4TM\text{-}5HT3A}$ (70.8 ± 3.2 and $64.6\pm2.9\%$, respectively) than for 5-HT$_{3A}{}^{3\text{-}4Loop\text{-}\alpha7}$ and 5-HT$_{3A}$ (90.7 ± 0.9 and $84.1\pm7.1\%$, respectively).

Considerable differences were also apparent in the noise variance of functional responses obtained with these subunit constructs, suggesting that regions outside of the four proposed transmembrane domains exert an influence upon ion channel properties (Figure 5 and Table 1). Previous

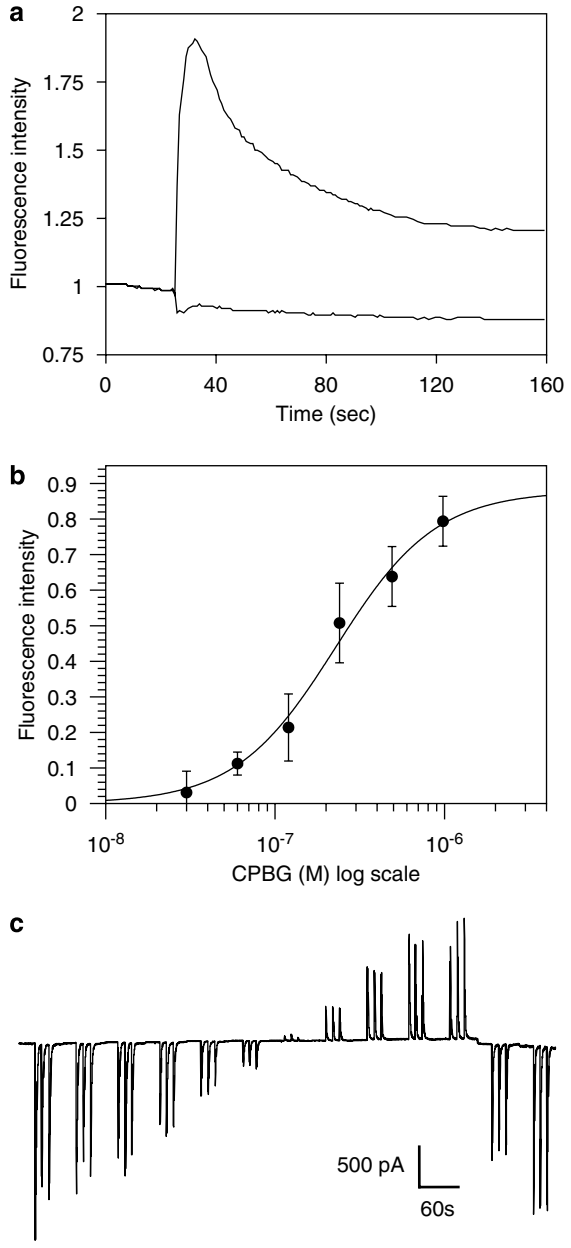

Figure 2 Functional characterization of subunit chimaeras by fluorescence imaging plate reader (FLIPR) and whole-cell electrophysiology. In all cases, representative data obtained with the 5-HT$_{3A}^{3\text{-}4\text{Loop-}\alpha7}$ chimaera are shown. (**a**) Elevation of intracellular calcium in transfected (upper trace) and mock-transfected (lower trace) tsA201 cells in response to agonist application (0.98 μM CPBG). The plot shows change in fluorescence intensity in cells plated in a 96-well plate loaded with the calcium-sensitive dye Fluo-4. (**b**) Dose–response curve constructed from fluorescence intensity measurements. Each data point is a mean of four wells of a 96-well plate in which the change in fluorescence detected in mock-transfected cells has been subtracted. (**c**) Whole-cell recording from tsA201 cells transfected with 5-HT$_{3A}^{3\text{-}4\text{Loop-}\alpha7}$. Agonist (1 μM CPBG) was applied for 500 ms, three times each minute. To obtain a current–voltage relation, the membrane potential was varied from −60 to +40 mV in 10 mV intervals and then returned to −40 mV and −60 mV. CPBG, 1-(3-chlorophenyl)biguanide hydrochloride.

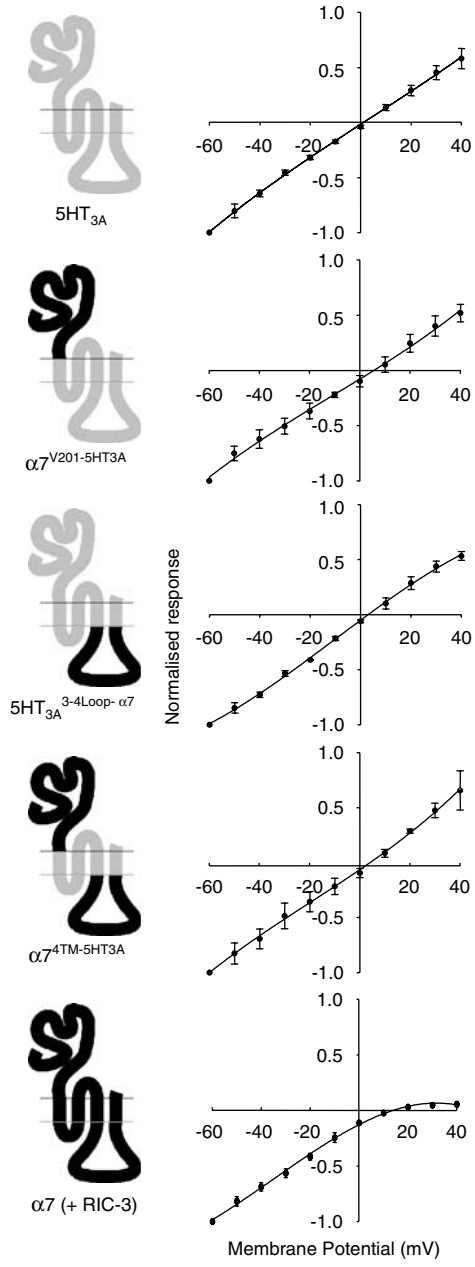

Figure 3 Influence of nAChR and 5-HT$_3$R subunit domains upon reversal potential and rectification. Wild-type and chimaeric subunits were expressed in tsA201 cells and analysed by whole-cell recording. Data with the nAChR α7 subunit were obtained in cells co-transfected with RIC-3. The current–voltage relations were obtained as described (see Methods and Figure 2c). Reversal potentials and rectification indices calculated from these data are shown in Table 1. nAChR, nicotinic acetylcholine receptor; 5-HT$_3$R, 5-hydroxytryptamine receptor type 3.

studies have reported that homomeric 5-HT$_{3A}$ receptors, produced by the heterologous expression of 5-HT$_{3A}$, exhibit very small (sub-pS) single-channel openings (Hussy *et al.*, 1994; Kelley *et al.*, 2003). Consistent with this is our observation that tsA201 cells expressing 5-HT$_{3A}$ generated whole-cell responses with little detectable noise during agonist application (Figure 5). Noise analysis of responses obtained with 5-HT$_{3A}$ gave a single-channel conductance of 0.7 ± 0.1 pS, ($n = 8$; Figure 5). The 5-HT$_{3A}^{3\text{-}4\text{Loop-}\alpha7}$ chimaera, in which the M3–M4 cytoplasmic loop of 5-HT$_{3A}$ is replaced with that of the α7 subunit, generated receptors with a

Table 1 Ion channel properties of α7/5-HT$_{3A}$ subunit constructs

Subunit	*Reversal potential (mV)*	*Rectification indices*		*Time constant for desensitization (ms)*		*Conductance (pS)*	
α7 (+RIC-3)	8.1±2.4	0.18±0.04	*	55±17	***	ND	
$\alpha7^{V201\text{-}5HT3A}$	4.8±2.6	0.94±0.08		223±32		0.8±0.1	***
$\alpha7^{4TM\text{-}5HT3A}$	6.6±2.4	1.01±0.15		925±220		30.5±4.0	***
5-HT$_{3A}$ $^{3\text{-}4Loop\text{-}\alpha7}$	5.8±2.6	1.08±0.04		7067±878		9.6±1.9	***
5-HT$_{3A}$	1.2±1.3	0.93±0.09		9201±1345		0.7±0.1	**

Abbreviation: 5-HT$_{3A}$, 5-hydroxytryptamine type 3A.
Reversal potential and rectification were calculated from the results shown in Figure 3. Data were fitted to a polynomial equation and the reversal potential was calculated. Rectification was then calculated as the ratio of the conductance at 40 – E_{rev} mV to the conductance at –60 – E_{rev} mV. Time constants for desensitization were derived from the results shown in Figure 4. Data were inverted and fitted with a one or the sum of two exponential functions ($I = I_{ss} + A^*e(-t/\tau)$, where I_{ss} = steady-state current, A = peak steady-state current, τ = time constant). From this, the time constants and the percentage desensitization after 20 s were calculated. Estimates of channel conductance were derived from noise spectral analysis (see Figure 5). Data are means of 5–10 independent recordings. *$P<0.05$, **$P<0.01$, ***$P<0.001$. ND = data not determined.

single-channel conductance of 9.6±1.9 pS ($n=11$), which is significantly higher than that of 5-HT$_{3A}$ ($P<0.05$). Analysis of whole-cell responses recorded from cells transfected with the $\alpha7^{V201\text{-}5HT3A}$ chimaera revealed a single-channel conductance of 0.8±0.1 pS ($n=5$), which is not significantly different from the sub-pS conductance observed with 5-HT$_{3A}$ (0.7±0.1 pS). Cells transfected with the $\alpha7^{4TM\text{-}5HT3A}$ chimaera expressed receptors with a single-channel conductance of 30.5±4.0 pS ($n=5$). This is significantly larger ($P<0.05$) than the conductance of receptors generated by the 5-HT$_{3A}$ $^{3\text{-}4Loop\text{-}\alpha7}$ chimaera and indicates that replacement of the extracellular domain of 5-HT$_{3A}$ with that of α7 leads to a significant increase in channel conductance (see Table 1).

As has been demonstrated previously, efficient functional expression of α7 nAChRs in mammalian cells lines such tsA201 requires co-expression of the nAChR-associated protein RIC-3 (Lansdell *et al*., 2005). Therefore, to enable the functional properties of 5HT$_{3A}$ and the α7/5HT$_{3A}$ chimaeras to be compared with α7 nAChRs, the α7 subunit was co-expressed with RIC-3 and examined by whole-cell recording. The reversal potential, determined from current–voltage relations in cells expressing α7 nAChRs (Figure 3), was similar to the reversal potential determined with the α7/5HT$_{3A}$ chimaeras and with 5HT$_{3A}$ (Table 1). Much greater rectification was observed with α7 than with any of the chimaeras or with 5HT$_{3A}$ (Figure 3, Table 1). The α7 responses showed complete desensitization, with a steady-state level of desensitization of 99.9±0.6%, $n=7$ (Figure 5). As expected, α7 responses desensitized very rapidly (Figure 5), which precluded a reliable estimate of single-channel conductance by noise analysis. The time constant for desensitization of α7 was significantly smaller ($P<0.001$) than the values obtained with either 5HT$_{3A}$ or the three chimaeras (Figure 4, Table 1).

Discussion

Difficulties in the efficient expression of functional α7 nAChRs in many heterologous expression systems have been a considerable hindrance to the detailed study. Evidence that subunit chimaeras containing the extracellular domain of the nAChR α7 subunit fused to the C-terminal domain of the 5-HT$_3$R subunit 5-HT$_{3A}$ (Eiselé *et al*., 1993) has been widely exploited by several research groups as a means of circumventing difficulties in heterologous expression of α7 (Eiselé *et al*., 1993; Blumenthal *et al*., 1997; Rangwala *et al*., 1997; Cooper and Millar, 1998). In a previous study aimed at identifying subunit domains influencing the folding and assembly of the α7 protein, it was concluded that inefficient folding and assembly could be attributed, in part, to regions close to the M1 hydrophobic transmembrane domain (Dineley and Patrick, 2000). Our findings are in agreement with this conclusion but also provide evidence that transmembrane domains other than M1 have a profound influence upon the efficiency of subunit folding. Only those subunit chimaeras in which all four α7 transmembrane domains were replaced with the corresponding regions from the 5-HT$_{3A}$ subunit were found to fold efficiently into a conformation which exhibited specific high-affinity binding of the nicotinic radioligand [^{125}I]αBTX and gave consistent agonist responses in whole-cell patch-clamp recordings.

In agreement with previous reports (Eiselé *et al*., 1993; Dineley and Patrick, 2000), our study confirms that inclusion of the TM1 domain of α7 within α7/5-HT$_{3A}$ subunit chimaeras results in an almost complete loss of [^{125}I]αBTX binding (compare $\alpha7^{V201\text{-}5HT3A}$ and $\alpha7^{S235\text{-}5HT3A}$). An important conclusion of the present study is that levels of [^{125}I]αBTX binding equivalent to the high levels generated by $\alpha7^{V201\text{-}5HT3A}$ are observed only in chimaeras containing all four transmembrane domains from 5-HT$_{3A}$ (e.g. $\alpha7^{4TM\text{-}5HT3A}$). All chimaeras containing combinations of α7 and 5-HT$_{3A}$ transmembrane domains generated significantly lower, if any, specific [^{125}I]αBTX-binding sites (Figure 1). For example, $\alpha7^{1TM\text{-}5HT3A}$, which contains only the first transmembrane domain of 5-HT$_{3A}$, generated very low levels of [^{125}I]αBTX binding (~1% of that detected with $\alpha7^{V201\text{-}5HT3A}$). This finding does not, however, contradict the findings of a previous study by Dineley and Patrick (2000), which highlighted the importance of the TM1 domain. Dineley and Patrick (2000) reported specific binding of [^{125}I]αBTX to an α7 chimaera containing only the TM1 region of 5-HT$_{3A}$ (see their Figure 4B), but this construct generated levels of binding which were less than 4% of that seen with the $\alpha7^{V201\text{-}5HT3A}$ chimaera.

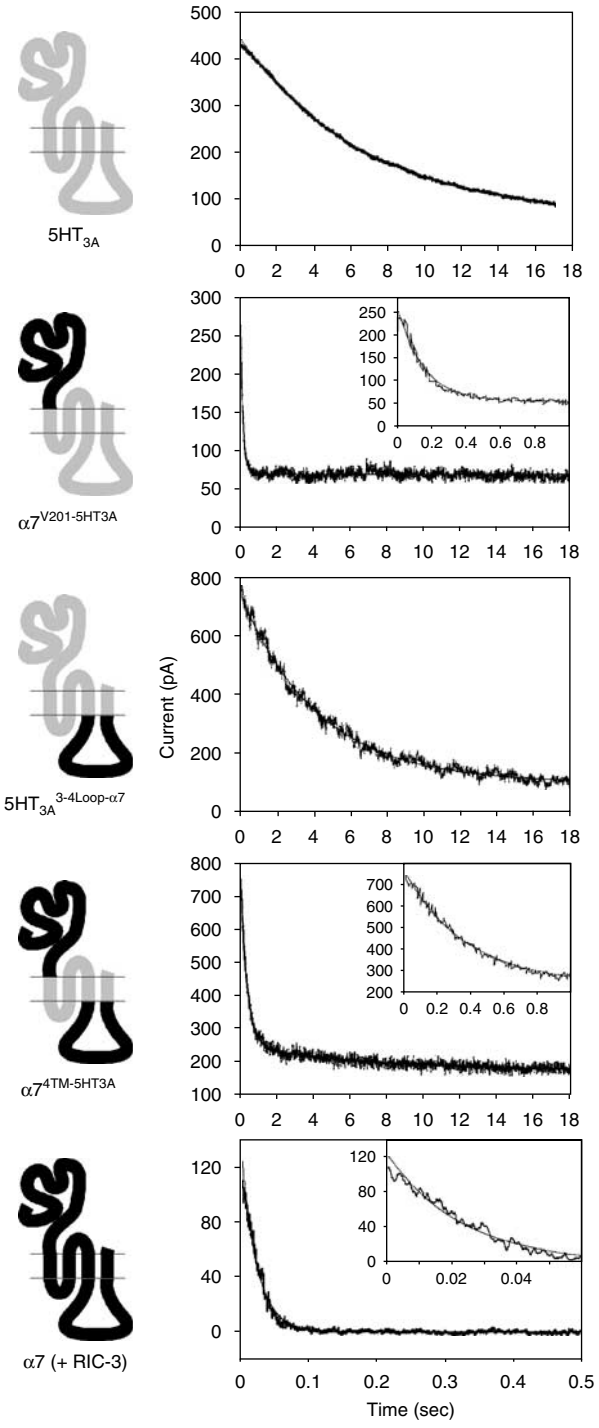

Figure 4 Influence of nAChR and 5-HT$_3$R subunit domains upon the kinetics of desensitization. Wild-type and chimaeric subunits were expressed in tsA201 cells and analysed by whole-cell recording. Data with the nAChR α7 subunit were obtained in cells co-transfected with RIC-3. Whole-cell responses obtained by a 20 s agonist application of either 200 or 20 μM DMPP (for α7, $\alpha7^{V201\text{-}5HT3A}$ and $\alpha7^{4TM\text{-}5HT3A}$) or 1 μM 5-HT (for 5-HT$_{3A}$ and 5-HT$_{3A}^{3\text{-}Loop\text{-}\alpha7}$). From these data, the time constants and the percentage desensitization after 20 s were calculated, as shown in Table 1. The insets show, on an expanded timescale, the fit to the initial part of the response desensitization. nAChR, nicotinic acetylcholine receptor; 5-HT$_3$R, 5-hydroxytryptamine receptor type 3; DMPP, 1,1-dimethyl-4-phenyl-piperazinium iodide.

There is strong evidence that the α7 subunit is able to form functional native nAChRs in neurones (Gray *et al*., 1996; Jones and Yakel, 1997; Yu and Role, 1998) and in some cultured mammalian cell lines (Puchacz *et al*., 1994; Gopalakrishnan *et al*., 1995; Quik *et al*., 1996). It seems likely therefore that problems encountered in its heterologous expression in several other cultured cell lines might be a consequence of these cells lacking one or more proteins required for assembly or trafficking. If this is the case, the present study would suggest that it is sequences present within the transmembrane domains of α7, rather than the main extracellular or intracelllular domains, which are responsible primarily for this requirement. Recent evidence has indicated that difficulties in the efficient expression of α7 in some cultured mammalian cell lines may be due to a requirement for the nAChR-associated protein RIC-3 (Castillo *et al*., 2005; Lansdell *et al*., 2005; Williams *et al*., 2005), a protein originally identified in *Caenorhabditis elegans* as the protein encoded by the gene 'resistance to inhibitors of cholinesterase' (Halevi *et al*., 2002). The present study suggests that in the absence of RIC-3, the transmembrane regions of α7 are responsible for inefficient folding and cell-surface expression. We also have obtained evidence which indicates that, in contrast to the situation with the α7 subunit (Lansdell *et al*., 2005), co-expression of RIC-3 with chimaeras containing regions of both the α7 and 5-HT$_{3A}$ subunits results in reduced levels of cell-surface [^{125}I]αBTX binding. This is consistent with previous studies which have examined the influence of RIC-3 on an α7/5-HT$_{3A}$ subunit chimaera (Castillo *et al*., 2005).

Differences in the efficiency with which α7 and 5-HT$_{3A}$ subunits are able to generate functional cell-surface receptors might have been predicted to be influenced by regions such as their large cytoplasmic M3–M4 domain. This region of nAChR subunits has been shown to interact with a range of intracellular proteins (Maimone and Enigk, 1999; Jeanclos *et al*., 2001; Lin *et al*., 2002) and to influence receptor targeting (Williams *et al*., 1998). Previous studies have also revealed that levels of cell surface expression can be modulated by sequences present in the large M3–M4 intracellular loop of nAChR subunits (Mishina *et al*., 1985; Yu and Hall, 1994; Valor *et al*., 2002). In contrast, our findings suggest that it is the four transmembrane regions, rather than the M3–M4 intracellular loop, which are primarily responsible for inefficient folding, assembly and cell-surface expression of α7 in many mammalian cell types.

As has been reported previously, there are examples of chimaeric nAChR subunits which form high-affinity nicotinic ligand-binding sites but for which functional channels cannot be detected (Campos-Caro *et al*., 1996; Campos-Caro *et al*., 1997). In the present study, we observed functional expression (using either whole-cell patch clamp recording or intracellular calcium assays) with all constructs for which high levels of radioligand binding was detected (and did not detect clear evidence of function channels with constructs for which little or no binding was detected). In most instances, the ion channel properties of subunits examined agreed with what might have been predicted from the subunit domains present. For example, chimaeric subunits containing all four transmembrane domains from 5-HT$_{3A}$

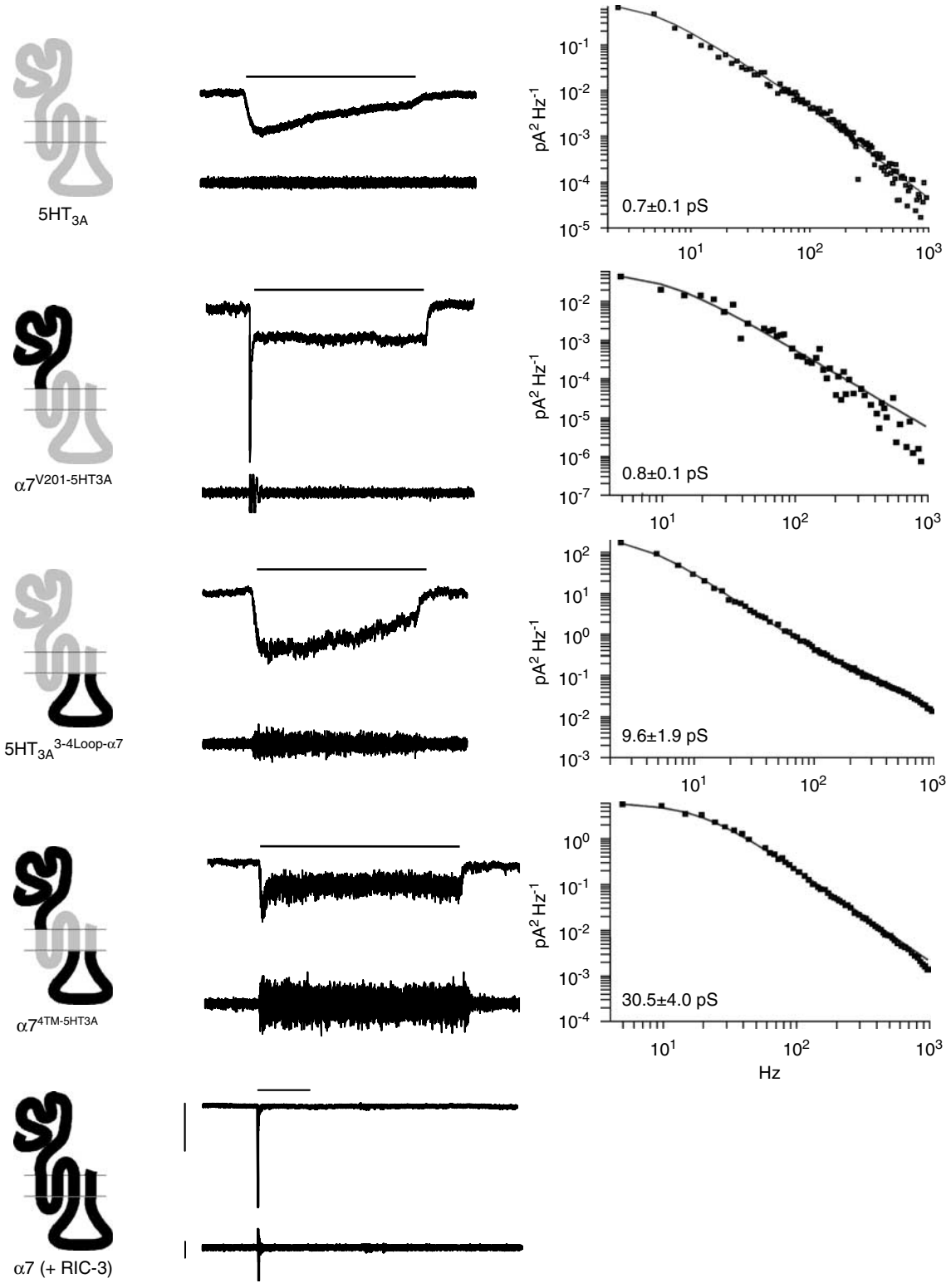

Figure 5 Influence of nAChR and 5-HT$_3$R subunit domains upon single-channel conductance. Wild-type and chimaeric subunits were expressed in tsA201 cells and analysed by whole-cell recording. Data with the nAChR α7 subunit were obtained in cells co-transfected with RIC-3. Representative whole-cell responses obtained by a 20 s application, or 0.5 s application in the case of α7 (horizontal bar) of either 200 or 20 μM DMPP (for α7, $\alpha7^{V201\text{-}5HT3A}$ and $\alpha7^{4TM\text{-}5HT3A}$) or 1 μM 5-HT (for 5-HT$_{3A}$ and 5-HT$_{3A}{}^{3\text{-}Loop\text{-}\alpha7}$). Horizontal scale bars = 20 s (5 s for α7), vertical scale bars = 100 pA. Below each whole-cell response is shown a high-gain band-pass filtered (2 Hz–2kHz) record illustrating the increase in noise variance associated with each response. Vertical scale bars = 20 pA. Representative plots illustrating the noise power spectrum for each chimaera are also shown. Due to very rapid desensitization, it was not possible to obtain a reliable estimate of single-channel conductance for α7 by noise analysis. Estimates of channel conductance were derived from noise spectral analysis of 5–10 cells (see Table 1) and were not significantly different from those estimated by analysis of plots of variance against mean current (not shown). nAChR, nicotinic acetylcholine receptor; 5-HT$_3$R, 5-hydroxytryptamine receptor; DMPP, 1,1-dimethyl-4-phenylpiperazinium iodide.

($\alpha7^{V201\text{-}5HT3A}$, $\alpha7^{4TM\text{-}5HT3A}$ and $5\text{-}HT_{3A}{}^{3\text{-}4Loop\text{-}\alpha7}$) exhibited rectification properties and reversal potentials which were similar to that of the wild-type 5-HT_{3A} subunit (Figure 3 and Table 1) and which differed substantially from recombinant α7 nAChRs (Couturier *et al*., 1990). In previous studies, slightly greater levels of rectification have been observed for $5HT_{3A}$ (Gunthorpe *et al*., 2000). It is possible that this may be a consequence of differences in the recording solutions used. For example, the intracellular solution used by Gunthorpe *et al*. contained 1 mM Mg^{2+}, whereas Mg^{2+} was absent from the intracellular solution used in the present study. Both 5-HT_{3A} and the $5\text{-}HT_{3A}{}^{3\text{-}4Loop\text{-}\alpha7}$ chimaera exhibited relatively slow rates of desensitization, as expected from previous studies of native 5-HT_3Rs (Mott *et al*., 2001). The decay time constants for 5-HT_{3A} and $5\text{-}HT_{3A}{}^{3\text{-}4Loop\text{-}\alpha7}$ (7067 ± 878 and 11277 ± 2023 ms, respectively) are not significantly different but are both significantly slower than for chimaeras containing an α7 extracellular domain ($\alpha7^{V201\text{-}5HT3A}$ and $\alpha7^{4TM\text{-}5HT3A}$; Figure 4 and Table 1). In this respect, the $\alpha7^{V201\text{-}5HT3A}$ and $\alpha7^{4TM\text{-}5HT3A}$ chimaeras resemble the rapid desensitization of wild-type α7 nAChRs (Couturier *et al*., 1990). This result is surprising, given the importance of residues in the M2 domain to desensitization of α7 nAChRs (Revah *et al*., 1991).

An important finding to emerge from this study is evidence that subunit domains other than the putative transmembrane regions have a significant influence upon single-channel conductance. Extensive experimental evidence exists to suggest that the M2 domain of ligand-gated ion channels lines the channel pore and exerts a direct influence upon ion channel properties. Residues within the M2 region of the *Torpedo* nAChR can be photo-affinity labelled by channel blockers (Giraudat *et al*., 1986; Hucho *et al*., 1986). The influence of residues within the nAChR M2 domain upon ion channel properties has been demonstrated by construction of subunit chimaeras (Imoto *et al*., 1986) and by site-directed mutagenesis (Imoto *et al*., 1988; Leonard *et al*., 1988; Charnet *et al*., 1990; Villarroel *et al*., 1991). The importance of the M2 domain in determining ion channel properties such as single-channel conductance and ion selectivity is supported by studies that have been conducted with other members of the Cys-loop receptor family (Bormann *et al*., 1993; Gunthorpe and Lummis, 2001). Evidence obtained from the series of subunit chimaeras described here demonstrates that single-channel conductance can be influenced by regions other than the predicted transmembrane regions. That the cytoplasmic M3–M4 loop domain of the nAChR α7 subunit can influence channel conductance agrees with a recent investigation of the 5-HT_3 receptor channel conductance which examined chimaeras constructed between the 5-HT_{3A} and 5-HT_{3B} subunits (Kelley *et al*., 2003). The present findings and other recently published studies on $\alpha4\beta2$ nAChRs (Hales *et al*., 2006) suggest that this is likely to be a general property of the nAChR superfamily. Kelley *et al*. (2003) demonstrated that three arginine residues within the M3–M4 loop of 5-HT_{3A} contributed to the low single-channel conductance of 5-HT_{3A} receptors. Our results fully support this conclusion, since the analogous amino acids in both human 5-HT_{3B} (Kelley *et al*., 2003) and rat α7 (this study) are either negatively charged (aspartic acid or glutamic acid) or uncharged (alanine, serine or glutamine). In addition, we have obtained evidence in the present study that conductance can also be influenced by the extracellular N-terminal domain of ligand-gated ion channels. It appears, however, that the intracellular loop domain contributes a greater initial rate-limiting effect on conductance than the extracellular domain. This is illustrated by the differences in conductance between $5HT_{3A}$ and $5HT_{3A}{}^{3\text{-}4Loop\text{-}\alpha7}$, and also between $\alpha7^{V201\text{-}5HT3A}$ and $\alpha7^{4TM\text{-}5HT3A}$. However, the extracellular domain can exert an additional effect on conductance, but only after this initial rate-limiting effect has been removed. This is illustrated by the differences in conductance between $5HT_{3A}{}^{3\text{-}4Loop\text{-}\alpha7}$ and $\alpha7^{4TM\text{-}5HT3A}$, and by the similarity in conductance between $5HT_{3A}$ and $\alpha7^{V201\text{-}5HT3A}$. It would appear, therefore, that multiple subunit domains, perhaps by allosteric conformational changes, are able to influence the rate of ion permeation through the channel.

In conclusion, the main findings of the present study concern the identification of nAChR and $5HT_3$R subunit domains which influence ion channel properties and efficiency of heterologous expression. We conclude that the widely reported problems associated with inefficient functional expression of α7 nAChR in the absence of the associated protein RIC-3 are due to the α7 transmembrane domains. In addition to the well-established evidence that single-channel conductance is influenced by the pore-forming M2 domain, our data support recent evidence that ion channel conductance can be influenced by intracellular domains. Our data extend these findings by demonstrating that extracellular subunit domains are also able to influence single-channel conductance.

Acknowledgements

This work was supported by grants from the Wellcome Trust. VJG and SK were supported by Wellcome Trust PhD studentships.

Conflict of interest

The authors state no conflict of interest.

References

Alexander SPH, Mathie A, Peters JA (2007). Guide to receptors and channels (GRAC), 2nd edition (2007 revision). *Br J Pharmacol* **150** (Suppl 1): S1–S168.

Baker ER, Zwart R, Sher E, Millar NS (2004). Pharmacological properties of α9α10 nicotinic acetylcholine receptors revealed by heterologous expression of subunit chimeras. *Mol Pharmacol* **65**: 453–460.

Blumenthal EM, Conroy WG, Romano SJ, Kassner PD, Berg DK (1997). Detection of functional nicotinic receptors blocked by α-bungarotoxin on PC12 cells and dependence of their expression on post-translational events. *J Neurosci* **17**: 6094–6104.

Bormann J, Rudström N, Betz H, Langosch D (1993). Residues within transmembrane segment M2 determine chloride conductance of glycine receptor homo- and hetero-oligomers. *EMBO J* **12**: 3729–3737.

Campos-Caro A, Rovira JC, Vincente-Agulló F, Ballesta JJ, Sala S, Criado M *et al*. (1997). Role of the putative transmembrane segment M3 in gating of neuronal nicotinic receptors. *Biochemistry* **36**: 2709–2715.

Campos-Caro A, Sala S, Ballesta JJ, Vincente-Agulló F, Criado M, Sala F (1996). A single residue in the M2–M3 loop is a major determinant of coupling between binding and gating in neuronal nicotinic receptors. *Proc Natl Acad Sci USA* **93**: 6118–6123.

Castillo M, Mulet J, Gutiérrez LM, Ortiz JA, Castelán F, Gerber S *et al*. (2005). Dual role of the RIC-3 protein in trafficking of serotonin and nicotinic acetylcholine receptors. *J Biol Chem* **280**: 27062–27068.

Charnet P, Labarca C, Leonard RJ, Vogelaar NJ, Czyzyk L, Gouin A *et al*. (1990). An open-channel blocker interacts with adjacent turns of α-helices in the nicotinic acetylcholine receptor. *Neuron* **2**: 87–95.

Chen D, Patrick JW (1997). The α-bungarotoxin-binding nicotinic acetylcholine receptor from rat brain contains only the α7 subunit. *J Biol Chem* **272**: 24024–24029.

Clarke PBS (1992). The fall and rise of neuronal α-bungarotoxin binding proteins. *Trends Pharmacol Sci* **13**: 407–413.

Cooper ST, Harkness PC, Baker ER, Millar NS (1999). Upregulation of cell-surface α4β2 neuronal nicotinic receptors by lower temperature and expression of chimeric subunits. *J Biol Chem* **274**: 27145–27152.

Cooper ST, Millar NS (1997). Host cell-specific folding and assembly of the neuronal nicotinic acetylcholine receptor α7 subunit. *J Neurochem* **68**: 2140–2151.

Cooper ST, Millar NS (1998). Host cell-specific folding of the neuronal nicotinic receptor α8 subunit. *J Neurochem* **70**: 2585–2593.

Couturier S, Bertrand D, Matter JM, Hernandez MC, Bertrand S, Millar N *et al*. (1990). A neuronal nicotinic acetylcholine receptor subunit (α7) is developmentally regulated and forms a homo-oligomeric channel blocked by α-BTX. *Neuron* **5**: 847–856.

Dempster J (2001). *The Laboratory Computer: a Practical Guide for Physiologists and Neuroscientists*. Academic Press: London.

Dineley KT, Patrick JW (2000). Amino acid determinants of α7 nicotinic acetylcholine receptor surface expression. *J Biol Chem* **275**: 13974–13985.

Drisdel RC, Green WN (2000). Neuronal α-bungarotoxin receptors are α7 subunit homomers. *J Neurosci* **20**: 133–139.

Eiselé J-L, Bertrand S, Galzi J-L, Devillers-Thiéry A, Changeux J-P, Bertrand D (1993). Chimaeric nicotinic–serotonergic receptor combines distinct ligand binding and channel specificities. *Nature* **366**: 479–483.

Giraudat J, Dennis M, Heidmann T, Chang J-Y, Changeux J-P (1986). Structure of the high-affinity binding site for noncompetitive blockers of the acetylcholine receptor: serine-262 of the δ subunit is labeled by [^{3}H]chlorpromazine. *Proc Natl Acad Sci USA* **83**: 2719–2732.

Gopalakrishnan M, Buisson B, Touma E, Giordano T, Campbell JE, Hu IC *et al*. (1995). Stable expression and pharmacological properties of the human α7 nicotinic acetylcholine receptor. *Eur J Pharmacol* **290**: 237–246.

Gray R, Rajan AS, Radcliffe KA, Yakehiro M, Dani JA (1996). Hippocampal synaptic transmission enhanced by low concentrations of nicotine. *Nature* **383**: 713–716.

Gunthorpe MJ, Lummis SCR (2001). Conversion of the ion selectivity of the 5-HT$_{3A}$ receptor from cationic to anionic reveals a conserved feature of the ligand-gated ion channel superfamily. *J Biol Chem* **276**: 10977–10983.

Gunthorpe MJ, Peters JA, Gill CH, Lambert JJ, Lummis SCR (2000). The 4′lysine in the putative channel lining domain affects desensitization but not the single-channel conductance of recombinant homomeric 5-HT$_{3A}$ receptors. *J Physiol* **522**: 187–198.

Hales TG, Dunlop JI, Deeb TZ, Carland JE, Kelley SP, Lambert JJ *et al*. (2006). Common determinants of single channel conductance within the large cytoplasmic loop of 5-hydroxytryptamine type 3 and α4β2 nicotinic acetylcholine receptors. *J Biol Chem* **281**: 8062–8071.

Halevi S, McKay J, Palfreyman M, Yassin L, Eshel M, Jorgensen EM *et al*. (2002). The *C. elegans ric-3* gene is required for maturation of nicotinic acetylcholine receptors. *EMBO J* **21**: 1012–1020.

Hargreaves AC, Lummis SCR, Taylor CW (1994). Ca^{2+} permeability of cloned and native 5-hydroxytryptamine type 3 receptors. *Mol Pharmacol* **46**: 1120–1128.

Hucho F, Oberthür W, Lottspeich F (1986). The ion channel of the nicotinic acetylcholine receptor is formed by the homologous helices MII of the receptor subunits. *FEBS Lett* **205**: 137–142.

Hussy N, Lukas W, Jones KA (1994). Functional properties of a cloned 5-hydroxytryptamine ionotropic receptor subunit: comparison with native mouse receptors. *J Physiol* **481**: 311–323.

Imoto K, Busch C, Sakmann B, Mishina M, Konno T, Nakai J *et al*. (1988). Rings of negatively charged amino acids determine the acetylcholine receptor channel conductance. *Nature* **335**: 645–648.

Imoto K, Methfessel C, Sakmann B, Mishina M, Mori Y, Konno T *et al*. (1986). Location of a δ-subunit region determining ion transport through the acetylcholine receptor channel. *Nature* **324**: 670–674.

Jeanclos EM, Lin L, Treuil MW, Rao J, DeCoster MA, Anand R (2001). The chaperone protein 14-3-3η interacts with the nicotinic acetylcholine receptor α4 subunit. *J Biol Chem* **276**: 28281–28290.

Jones S, Yakel JL (1997). Functional nicotinic ACh receptors on interneurones in the rat hippocampus. *J Physiol* **504**: 603–610.

Kassner PD, Berg DK (1997). Differences in the fate of neuronal acetylcholine receptor protein expressed in neurons and stably transfected cells. *J Neurobiol* **33**: 968–982.

Kelley SP, Dunlop JI, Kirkness EF, Lambert JJ, Peters JA (2003). A cytoplasmic region determines single-channel conductance in 5-HT$_3$ receptors. *Nature* **424**: 321–324.

Lansdell SJ, Gee VJ, Harkness PC, Doward AI, Baker ER, Gibb AJ *et al*. (2005). RIC-3 enhances functional expression of multiple nicotinic acetylcholine receptor subtypes in mammalian cells. *Mol Pharmacol* **68**: 1431–1438.

Lansdell SJ, Millar NS (2004). Molecular characterisation of Dα6 and Dα7 nicotinic acetylcholine receptor subunits from *Drosophila*: formation of a high-affinity α-bungarotoxin binding site revealed by expression of subunit chimeras. *J Neurochem* **90**: 479–489.

Le Novère N, Corringer P-J, Changeux J-P (2002). The diversity of subunit composition in nAChRs: evolutionary origins, physiologic and pharmacologic consequences. *J Neurobiol* **53**: 447–456.

Leonard RJ, Labarca CG, Charnet P, Davidson N, Lester HA (1988). Evidence that the M2 membrane-spanning region lines the ion channel pore of the nicotinic receptor. *Science* **242**: 1578–1581.

Lin L, Jeanclos EM, Treuil MW, Braunewell K-H, Gundelfinger ED, Anand R (2002). The calcium sensor protein visinin-like protein-1 modulates the surface expression and agonist-sensitivity of the α4β2 nicotinic acetylcholine receptor. *J Biol Chem* **277**: 41872–41878.

MacDermott AB, Role LW, Sigelbaum SA (1999). Presynaptic ionotropic receptors and the control of transmitter release. *Annu Rev Neurosci* **22**: 443–485.

Maimone MM, Enigk RE (1999). The intracellular domain of the nicotinic acetylcholine receptor a subunit mediates its cocluster-ing with rapsyn. *Mol Cell Neurosci* **14**: 340–354.

Maricq AV, Peterson AS, Brake AJ, Myers RM, Julius D (1991). Primary structure and functional expression of the 5HT$_3$ receptor, a serotonin-gated ion channel. *Science* **254**: 432–437.

Millar NS (2003). Assembly and subunit diversity of nicotinic acetylcholine receptors. *Biochem Soc Trans* **31**: 869–874.

Mishina M, Tobimatsu T, Tanaka K, Fujita Y, Fukuda K, Kurasake M *et al*. (1985). Location of functional regions of acetylcholine receptor α-subunit by site-directed mutagenesis. *Nature* **313**: 364–369.

Mott DD, Erreger K, Banke TG, Traynelis SF (2001). Open probability of homomeric murine 5-HT$_{3A}$ serotonin receptors depends on subunit occupancy. *J Physiol* **535**: 427–443.

Puchacz E, Buisson B, Bertrand D, Lukas RL (1994). Functional expression of nicotinic acetylcholine receptors containing rat α7 subunits in human SH-SY5Y neuroblastoma cells. *FEBS Lett* **354**: 155–159.

Quik M, Choremis J, Komourian J, Lukas RJ, Puchacz E (1996). Similarity between rat brain nicotinic α-bungarotoxin receptors and stably expressed α-bungarotoxin binding sites. *J Neurochem* **67**: 145–154.

Quiram PA, Sine SM (1998). Identification of residues in the neuronal α7 acetylcholine receptor that confer selectivity for conotoxin ImI. *J Biol Chem* **273**: 11001–11006.

Rangwala F, Drisdel RC, Rakhilin S, Ko E, Atluri P, Harkins AB *et al*. (1997). Neuronal α-bungarotoxin receptors differ structurally from other nicotinic acetylcholine receptors. *J Neurosci* **17**: 8201–8212.

Revah F, Bertrand D, Galzi JL, Devillers-Thiery A, Mulle C, Hussy N *et al*. (1991). Mutations in the channel domain alter desensitization of a neuronal nicotinic receptor. *Nature* **353**: 846–849.

Séguéla P, Wadiche J, Dineley-Miller K, Dani JA, Patrick JW (1993). Molecular cloning, functional properties, and distribution of rat brain α7: a nicotinic cation channel highly permeable to calcium. *J Neurosci* **13**: 596–604.

Valor LM, Mulet J, Sala F, Ballesta JJ, Criado M (2002). Role of the large cytoplasmic loop of the α7 neuronal nicotinic acetylcholine receptor subunit in the receptor expression and function. *Biochem* **41**: 7931–7938.

Villarroel A, Herlitze S, Koenen M, Sakmann B (1991). Location of a threonine residue in the α-subunit M2 transmembrane segment that determines the ion flow through the acetylcholine receptor channel. *Proc R Soc Lond B* **243**: 69–74.

Williams BM, Temburni MK, Levey MS, Bertrand S, Bertrand D, Jacob MH (1998). The long internal loop of the α3 subunit targets nAChRs to subdomains within individual synapses on neurones *in vivo*. *Nat Neurosci* **1**: 557–562.

Williams ME, Burton B, Urrutia A, Shcherbatko A, Chavez-Noriega LE, Cohen CJ *et al*. (2005). Ric-3 promotes functional expression of the nicotinic acetylcholine receptor α7 subunit in mammalian cells. *J Biol Chem* **280**: 1257–1263.

Yu CR, Role LW (1998). Functional contribution of the α7 subunit to multiple subtypes of nicotinic receptors in embryonic chick sympathetic neurones. *J Physiol* **509**: 651–665.

Yu X-M, Hall ZW (1994). A sequence in the main cytoplasmic loop of the α subunit is required for assembly of mouse muscle nicotinic acetylcholine receptor. *Neuron* **13**: 247–255.

Zhao L, Kuo Y-P, George AA, Peng J-H, Purandare MS, Schroeder KM *et al*. (2003). Functional properties of homomeric, human α7-nicotinic acetylcholine receptors heterologously expressed in the SH-EP1 human epithelial cell line. *J Pharmacol Exp Ther* **305**: 1132–1141.